BASHY Dyes Are Highly Efficient Lipid Droplet-targeting Photosensitizers That Induce Ferroptosis Through Lipid Peroxidation

Maria J. S. A. Silva,[a,b],# Yiyi Zhang,[b],# Robin Vinck,[b] Fábio M. F. Santos,[a] João P. M. António,[a] Lisa Gourdon-Grünewaldt,[b,c] Charlotte Zaouter,[c] Annie Castonguay,[c] Shunmoogum A. Patten,[c] Kevin Cariou,[b] Francisco Boscá,[d] Francisco Nájera,[e] Jesús F. Arteaga,[f] Gilles Gasser,[b]* Uwe Pischel,[f]* Pedro M. P. Gois[a]*

[a] Dr. M. J. S. A. Silva, Dr. F. M. F. Santos, Dr. J. P. M. António, Prof. Dr. P. M. P. Gois
Research Institute for Medicines (iMed.ULisboa)
Faculdade de Farmácia, Universidade de Lisboa
Lisboa, Portugal
E-mail: pedrogois@ff.ulisboa.pt

[b] Dr. M. J. S. A. Silva, Y. Zhang, Dr. R. Vinck, L. Gourdon-Grünewaldt, Dr. K. Cariou, Prof. Dr. G. Gasser
Institute of Chemistry for Life and Health Sciences, Laboratory for Inorganic Chemical Biology
Institution Chimie ParisTech, PSL University CNRS
F-75005 Paris, France
E-mail: gilles.gasser@chimieparistech.psl.eu

[c] L. Gourdon-Grünewaldt, C. Zaouter, Dr. A. Castonguay, Dr. S. A. Patten
INRS - Institut Armand-Frappier
Université du Québec
531 boul. des Prairies, Laval, Quebec, H7V 1B7, Canada

[d] Dr. F. Boscá
Instituto de Tecnología Química
Universitat Politècnica de València – Consejo Superior de Investigaciones Científicas
Avda. de los Naranjos s/n, 46022 Valencia, Spain

[e] Prof. Dr. F. Nájera
Departamento de Química Orgánica, and Instituto de Investigación Biomédica de Málaga y Plataforma en Nanomedicina – IBIMA
Universidad de Málaga
Campus Teatinos s/n, 29071, Plataforma Bionand, Parque Tecnológico de Andalucía, 29590 Málaga, Spain

[f] Prof. Dr. J. F. Arteaga, Prof. Dr. U. Pischel
CIQSO-Centre for Research in Sustainable Chemistry and Department of Chemistry
University of Huelva
Campus de El Carmen s/n, 21071, Huelva, Spain
E-mail: uwe.pischel@diq.uhu.es

# These authors have contributed equally to the work.

Supporting information for this article is given via a link at the end of the document

Abstract: Ferroptosis is an iron-dependent lipid peroxidation-driven mechanism of cell death and a promising therapeutic target to eradicate cancer cells. In this study we discovered that boronic acid derived salicylidenehydrazone (BASHY) dyes are highly efficient singlet-oxygen photosensitizers (PSs; Φ_{Δ} up to 0.8) that induce ferroptosis triggered by photodynamic therapy. The best performing BASHY dye displayed a high phototoxicity against the human glioblastoma multiform U87 cell line, with an IC_{50} value in the low nanomolar range (4.40 nM) and a remarkable phototoxicity index (PI > 22700). Importantly, BASHY dyes were shown to accumulate in lipid droplets and this intracellular partition was found to be essential for the enhanced phototoxicity and the induction of ferroptosis through lipid peroxidation. The safety and phototoxcity of this platform were validated in *in vivo* studies on zebrafish embryos (*Danio rerio*).

Introduction

A deeper understanding of the molecular mechanisms that govern cell death is fundamental to develop innovative therapeutic approaches. In this context, ferroptosis emerged in recent years as a very useful therapeutic target in cancer.[1] Ferroptosis is a non-apoptotic mode of cell death driven by iron-dependent lipid peroxidation and the current literature converges on suggesting an intimate relationship between this modality of cell death and an imbalanced redox homeostasis.[2] Recent studies point to the central role of lipid hydroperoxides (LOOH) in ferroptosis.[2–5] LOOH are then decomposed to form alkoxyl radicals (LO•) that initiate oxidative chain reactions of cell membrane phospholipids. This triggers uncontrolled lipid

https://doi.org/10.26434/chemrxiv-2023-03s0m ORCID: https://orcid.org/0000-0002-7698-630X Content not peer-reviewed by ChemRxiv. License: CC BY-NC-ND 4.0

peroxidation (LPO), leading ultimately to plasma membrane rupture and cell death.

Contrary to healthy cells, cancer cells exhibit an increased level of reactive oxygen species (ROS), which is indispensable to sustain the biochemical alterations required for the initiation and progression of the disease.[6] However, perturbation of this tightly regulated redox balance can result in the oxidation of important cellular components, ultimately leading to cell death by various mechanisms, including ferroptosis. Therefore, many efforts have been made to discover therapeutic approaches to selectively target this redox system. Among these strategies the use of photodynamic therapy (PDT) is particularly appealing,[7,8] because the activation of a photosensitizer (PS) by light can generate singlet oxygen which promotes LPO or produces hydrogen peroxide for intracellular Fenton reactions.[9] However, apart from a few recent examples,[10–12] most of the available PSs failed to effectively induce ferroptosis since phototoxicity can trigger different mechanisms of cell death, depending on the cell type, light intensity, and intracellular localization of the PS. Moreover, most reported ferroptosis-inducing PSs resort to supramolecular encapsulation in nanoparticles or liposomes to improve their cancer cell targeting and stability in circulation.[7] Therefore, the discovery of new PSs with improved accumulation in lipid-rich regions during PDT treatment would offer a powerful and highly selective strategy to induce ferroptotic pathways through localized LPO.

Recently, we developed a modular fluorescent platform based on boronic acid derived salicylidenehydrazone complexes (BASHY) that absorb at wavelengths >450 nm, display high molar absorption coefficients (up to 70000 $M^{-1}cm^{-1}$), and show polarity-dependent emission in the green-to-red spectral range.[13–18] More importantly, the hydrophobic BASHY dyes were shown to effectively accumulate in lipid droplets (LDs).[18] These structures are spherical cytoplasmic organelles composed of a neutral lipid core, that play a key role in tumor metabolism and act, among other functions, as lipid reserves to sustain the fast proliferation of cancer cells.[19] Therefore, we anticipated that if BASHY dyes would work as efficient PSs, this platform could become a unique tool to promote light-induced ferroptosis in cancer cells (Figure 1).

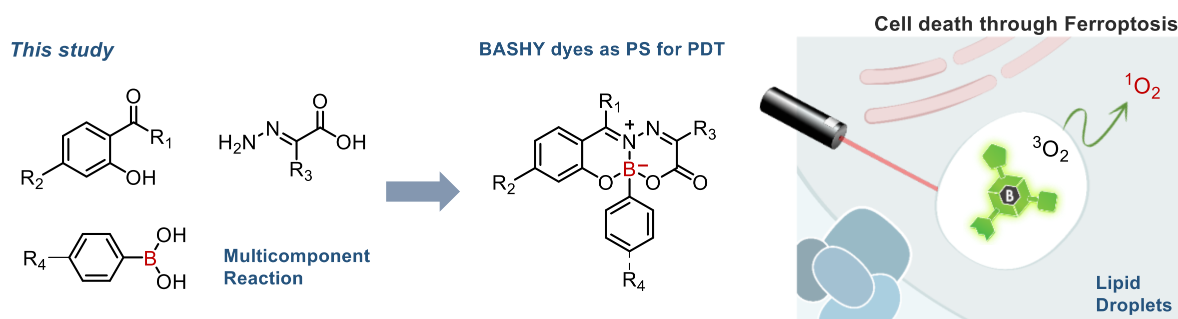

Figure 1. BASHY dyes as a new PS platform for PDT that targets lipid droplets and trigger ferroptosis.

Results and Discussion

To test this hypothesis, we prepared the BASHY dyes **1**–**3**[16,18] and studied their capacity to populate the excited triplet state and generate singlet oxygen. The architecture of the dyes was chosen to cover different levels of π-conjugation along the salicylidenehydrazone ligand backbone, which impacts the photo-physical and -chemical properties (see Table 1 and Supporting Information).[16] In addition to this series, dye **3** was equipped with a cholesterol moiety to induce a different partition of the dye among intracellular lipid rich regions and to study the impact of this partition in the PDT response of the dye. This yielded dye **4** for which representative photophysical data are shown in Figure 2 (the data for the dyes **1**–**3** can be found in the Supporting Information).

BASHY dyes are known to present a mixed character in terms of charge-transfer (CT) properties and a cyanine-like behaviour.[16,20] On the one hand, the latter has an increased contribution in BASHY dyes with extended π-conjugation, i.e., in the dyes **3** and **4**. On the other hand, the CT character is much more notable for the dyes **1** and **2**. This was corroborated by quantum-mechanical calculations (see Supporting Information). Furthermore, the CT process depends on the polarity of the solvent, i.e., more CT is anticipated in polar media (e.g., acetonitrile; ACN) than in a non-polar environment (e.g., toluene; TOL). Noteworthy, the integration of the cholesterol moiety in **4** does not alter the photophysical properties as compared to dye **3**. This is in accordance with our previous finding that the photophysics of BASHY dyes is principally governed by the electronic properties of the salicylidenehydrazone backbone.[15,17]

The dyes absorb with maxima at about 470 to 520 nm and, thus, can be conveniently excited in the visible spectral range by blue or green light. The absorption maximum is red-shifted with increasing degree of π-conjugation, according to the expectations on the cyanine-like character. In acetonitrile, the dyes emit fluorescence with maxima between 550 and 600 nm and show moderate quantum yields Φ_f (*ca.* 0.2–0.3). Upon changing the medium to toluene, the fluorescence maximum is blue-shifted due to a destabilization of the emissive CT state and the fluorescence quantum yield is increased as compared to the polar medium. This is especially notable for the dyes **1** and **2**, those having the more pronounced CT character.

https://doi.org/10.26434/chemrxiv-2023-03s0m **ORCID:** https://orcid.org/0000-0002-7698-630X Content not peer-reviewed by ChemRxiv. **License:** CC BY-NC-ND 4.0

Table 1. Photophysical data of the BASHY dyes **1**–**4** in acetonitrile and toluene solution.

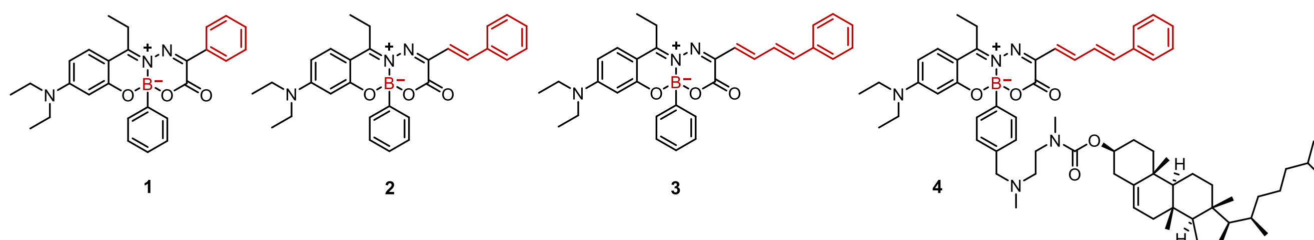

		λ_{abs} (nm)[a] [ε ($M^{-1}cm^{-1}$)]	λ_f (nm)[a]	Φ_f[a]	τ_f (ns)[a]	λ_{T-T} (nm)[b] [ε ($M^{-1}cm^{-1}$)]	τ_T (µs)[c]	Φ_{ISC}[d]	Φ_Δ[e]
1	ACN	472 [52000]	552	0.16	1.01	720 [9970]	43.5	0.10	0.08
	TOL	472 [49000]	509	0.72	2.52	750 [9970]	29.1	0.23	0.23
2	ACN	497 [58000]	577	0.26	1.72	680 [12135]	41.6	0.10	0.10
	TOL	497 [58000]	531	0.58	2.12	680 [12135]	20.6	0.20	0.22
3	ACN	513 [62000]	585	0.25	1.57	660 [12900]	23.5	0.48	0.33
	TOL	513 [60000]	548	0.32	1.18	690 [12900]	26.6	0.78	0.79
4	ACN	511 [62000]	585	0.15	1.69	660 [12830]	25.1	0.40	0.26
	TOL	514 [59000]	551	0.31	1.29	670 [12830]	16.3	0.75	0.82

[a] Data (except for dye **4**) are taken from ref.[16]; error of quantum yields ±15%; error of lifetimes ±5%. [b] Triplet-triplet absorption maximum (λ_{exc} = 355 nm); in square brackets the molar absorption coefficients at 670 nm are given; the values in toluene are assumed to be same as in acetonitrile. [c] Triplet lifetime in deaerated solution (λ_{exc} = 355 nm); error ±10%. [d] Intersystem crossing (ISC) quantum yield (λ_{exc} = 355 nm); error ±20%. [e] Quantum yield of singlet oxygen formation (λ_{exc} = 355 nm); reference perinaphthenone (Φ_Δ ($^1O_2$) = 0.98 in ACN); error ±20%.

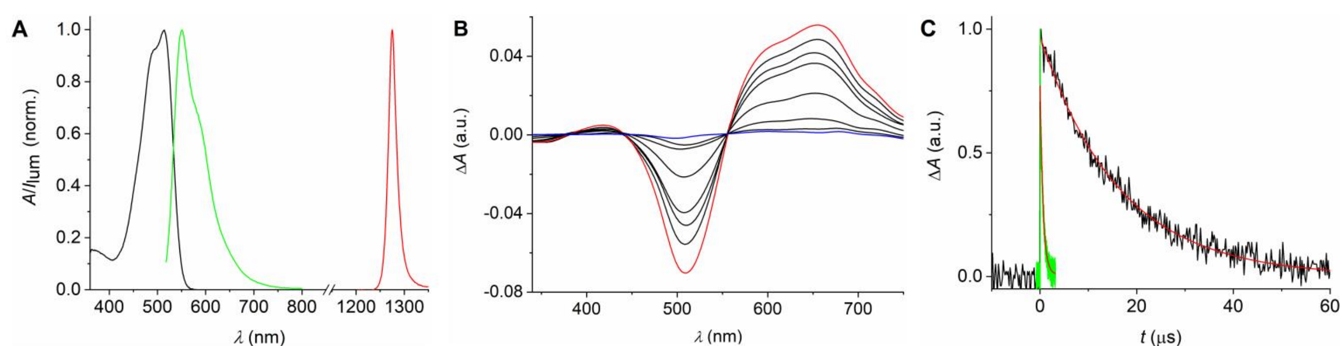

Figure 2. A) Absorption (black) and fluorescence (green) spectra of dye **4** in toluene. The NIR spectrum (red) shows the phosphorescence of the generated singlet oxygen. B) Nanosecond laser-flash photolysis spectra of dye **4** in deaerated acetonitrile (red: 2.2 µs after laser flash; blue: after 70.5 µs). C) Triplet decay under anaerobic (black) and aerobic conditions (green) and the respective monoexponential fitting (red).

As rated by the moderate fluorescence quantum yield of **3** and **4** it could be expected that the population of the excited triplet state via intersystem crossing (ISC) contributes significantly to the excited state trajectory. Indeed, such evidence for the excited triplet state population was obtained from nanosecond transient-absorption spectroscopy in oxygen-free solutions. The investigated dyes lead to transient states that absorb at wavelengths longer than 600 nm and show decay kinetics on the microsecond timescale (τ_T *ca.* 20–40 µs), see Figure 2B and C, Table 1, and the Supporting Information. These signals have been assigned to the triplet-triplet absorption. The intersystem crossing (ISC) quantum yields Φ_{ISC} of the dyes in acetonitrile vary between 0.1 (for dye **1**) and 0.48 (for dye **3**). In this solvent the values for Φ_{fluo} and Φ_{ISC} do not add up to one, which points to a significant decay of the excited singlet state via non-radiative pathways in acetonitrile, e.g., spin-allowed charge recombination (CR). This is prominently the case for the dyes **1** and **2**, which imply more significant CT contributions. Hence, the

https://doi.org/10.26434/chemrxiv-2023-03s0m ORCID: https://orcid.org/0000-0002-7698-630X Content not peer-reviewed by ChemRxiv. License: CC BY-NC-ND 4.0

competition between CR and ISC lowers the efficiency of excited triplet state population dramatically for these dyes. In toluene, where CT is rather disfavoured, a considerably more efficient ISC was noted, especially for the dyes **3** and **4** (Φ_{ISC} = 0.75–0.78), and partially also for the dyes **1** and **2**. From these observations it becomes clear that the presence of significant CT contributions apparently hinders an efficient ISC. Noteworthy, previously discussed ISC pathways under involvement of CT states, such as radical pair ISC or spin-orbit charge-transfer ISC,[21] seem not to be operative in these cases. The "purest" locally-excited triplet state is expected for the dyes **3** and **4** in toluene, which is in coincidence with the experimentally verified efficient ISC by a classical spin-orbit coupling mechanism. A qualitative picture of the involved photoprocesses is given in Scheme 1.

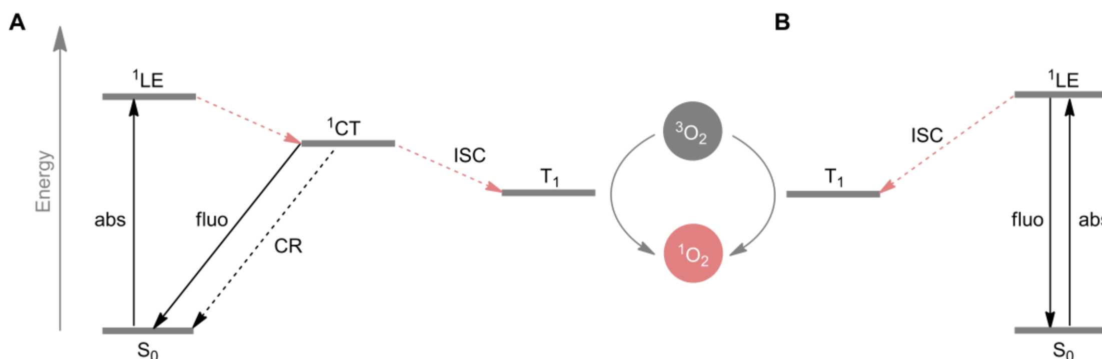

Scheme 1. General schemes with proposed photophysical pathways of (A) the dyes **1** and **2** as well as (B) **3** and **4**. Non-radiative processes are symbolized by dashed lines. LE: locally excited state; CT: charge transfer state; T: triplet state; ISC: intersystem crossing; CR: charge recombination; abs: absorption; fluo: fluorescence.

The excited triplet states show a dramatically reduced lifetime in the presence of oxygen (see Figure 2C), pointing to an efficient quenching process (bimolecular quenching rate constant of *ca.* 5 × 10^9 $M^{-1}s^{-1}$ for all dyes). One outcome of this quenching is the sensitization of $^1O_2$ by means of triplet energy transfer, as evidenced by the direct observation of its luminescence in the near-infrared spectral region (maximum at 1270 nm); see Figure 2. The quantum yields for $^1O_2$ formation (Φ_Δ) coincide, especially in non-polar medium (e.g., toluene), with those of the triplet-state population by ISC; see Table 1. This observation evidences a practically quantitative energy transfer process to $^3O_2$ and thereby a strong preference for the type II mechanism ($^1O_2$ formation instead of electron-transfer-induced formation of other reactive oxygen species) as cornerstone of the anticipated PDT activity (see below).[22] From the joint photophysical data it can be unambiguously concluded that the dyes **3** and **4**, i.e., those with the most pronounced cyanine-like character, are excellent candidates for PDT. Noteworthy, the herein established PSs do not require the presence of triplet-state promoting heavy atoms, such as bromine or iodine, which are often known to cause also an elevated dark toxicity.[23]

With the photophysical data in hand, we proceeded to evaluate the hydrolytic stability of compounds **1**–**3** (see Supporting Information). The extended conjugation appears to have a positive effect on their stability, with dye **3** displaying the highest aqueous stability with a half-life ($t_{1/2}$) of 43.3 h (*versus* 4.9 h for dye **1**). Moreover, in a non-aqueous environment (ACN), the three dyes displayed excellent stabilities with $t_{1/2}$ values between 46 h (dye **1**) and 138 h (dye **3**). In terms of the photostability these dyes present the typical light-induced oxidation patterns at the polymethine chain as reported for archetypal cyanine dyes (see Supporting Information).[24] Though the observed photobleaching has no detrimental effect on the PDT efficiency (see below).

We next addressed if the dyes are accumulating in LDs and if this partition could selectively enhance LPO and PDT-induced ferroptosis. Therefore, exploring the intrinsic fluorescence of the dye, we monitored the intracellular distribution of **3** in human glioblastoma multiforme U87 cells by confocal microscopy (Figure 3). As mentioned above, BASHY dyes are well-known to be selective markers for LDs.[18] In accordance with those reports, BASHY **3** displayed a preferred accumulation in globular intracellular organelles. After confirming this selective accumulation profile, we studied if these dyes could act as PSs in PDT assays. Hence, their phototoxicity was tested against U87 cells and non-cancerous human retinal pigment epithelial-1 (RPE-1) cells. As shown in Table 2, upon irradiation at 540 nm for 40 min (3.75 mW cm^{-2}; 9.50 J cm^{-2}) the dyes **1**–**3** showed elevated phototoxicity against U87 cells with IC_{50} values ranging from micro- to nanomolar concentrations. These numbers correlate well with the dyes' capacity to generate $^1O_2$ (see Table 1). Dye **3**, which exhibits one of the highest $\Phi_\Delta(^1O_2)$ of the series, proved to be the most potent PS in these assays (IC_{50} = 4.40 nM).

Gratifyingly, the dyes displayed no toxicity in the dark at concentrations of up to 100 μM, leading to an impressive phototoxicity index (PI) of >22700 for dye **3** and to some lesser extent also for dye **2** (PI > 3500). The figures contrast with those obtained with Protoporphyrin IX (PPIX), a standard PS used in clinical practice, and are amongst the highest reported PI values.[25,26] Under comparable experimental conditions as applied for the dyes **1**–**3**, PPIX shows an IC_{50} of only 521 nM against U87 cancer cells, leading to a rather poor PI of 9.5. Of note, dye **3** was found to be 3.4-fold more toxic in U87 cells than

https://doi.org/10.26434/chemrxiv-2023-03s0m **ORCID:** https://orcid.org/0000-0002-7698-630X Content not peer-reviewed by ChemRxiv. **License:** CC BY-NC-ND 4.0

in non-cancerous RPE-1 cells ($P < 0.0001$, t-test). In contrast, dye **2** was only 1.4-fold more toxic on U87 cells ($P < 0.01$, t-test), while no significant difference was observed for PPIX.

Table 2. Cytotoxicity (IC_{50} values) of tested compounds on U87 and RPE-1 cell lines in the dark or upon light irradiation.[a]

	${}^{dark}IC_{50}$ (μM)	${}^{light\ 540\ nm}IC_{50}$ (nM)[b]	PI[c]
U87 MG cell line			
1	>100	14260 ± 780	>7
2	>100	27.9 ± 1.5	>3600
3	>100	4.4 ± 0.2	>22700
4	>100	98 ± 17	>1000
PPIX	4.93 ± 1.18	521 ± 94	9.5
RPE-1 cell line			
1	>100	5740 ± 640	>17
2	>100	39.0 ± 2.9	>2500
3	>100	15.0 ± 1.0	>6700
4	>100	214 ± 10	>500
PPIX	6.11 ± 0.76	403 ± 19	15

[a] Cells were incubated with the compounds for 4 h before they were washed and the medium was replaced with fresh medium. Data are presented as means ± standard deviation (SD) of three independent replicates. [b] Irradiation at 540 nm (3.75 mW cm^{-2}, 9.50 J cm^{-2}). [c] The phototoxicity index (PI) is defined as the ratio ${}^{dark}IC_{50}/{}^{light540\ nm}IC_{50}$.

Once the capacity of **3** to act as a potent PS was established, we addressed the contribution of LDs to the efficiency of this dye. With this objective, dye **4** was designed based on the architecture of **3** and featuring an additional cholesterol unit. Cholesterol is well known for promoting accumulation in different intracellular lipidic regions.[27,28] Therefore, we anticipated that if **4** would display a differentiated intracellular distribution as compared to **3**, this would induce a modulation of the response in PDT.

We monitored the intracellular distribution of **4** by confocal microscopy in U87 cells (Figure 3). Differently from **3**, dye **4** did not show a marked preference for accumulation in LDs and was only partially found in these globular intracellular organelles. Next, U87 and RPE-1 cells were incubated with **4** and submitted to irradiation at 540 nm for 40 min. In these conditions, IC_{50} values of 98 nM and 214 nM against U87 and RPE-1 cells, respectively, were obtained. These results showcase a decrease (by *ca.* one order of magnitude) in PDT potency in comparison with dye **3**; however, the dark toxicity (>100 μM) remained low and the phototoxicity index (PI > 500) was still significant.

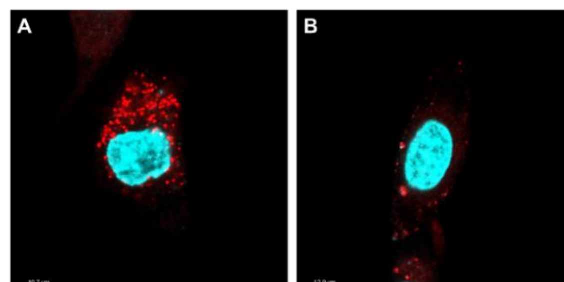

Figure 3. Live cell confocal microscopy image of U87 cells incubated with dyes **3** (A) and **4** (B). Cells were incubated with 500 nM dye for 3 h (red, excitation: 488 nm, emission: 597–651 nm) and the nuclear staining dye Hoechst 33342 (cyan, excitation: 405 nm, emission: 409–448 nm).

Together these results strongly suggest that the prominent accumulation of **3** in LDs results in a more efficient cell death. To further test this hypothesis, inductively coupled plasma mass spectrometry (ICP-MS) studies were performed on U87 cells to determine the cellular and LD uptake of both dyes **3** and **4**. As shown in Figure 4, the cellular uptake of **3** is about 3-fold higher than that observed for **4**. More importantly, within 1–4 h, approximately one-third of the intracellular concentration of **3** or **4** is localized in LDs, and this uptake clearly increases over time. However, because dye **4** shows a limited accumulation in cells, its absolute amount in LDs is consequently rather low. These observations support the hypothesis that the higher phototoxicity observed with **3** is directly linked to the higher concentration of the dye in lipid-rich organelles. It must be stressed here that the nonpolar surrounding that is provided in LDs boosts the performance of the PS in terms of ${}^1O_2$ generation, as discussed above for the photophysical model studies in toluene. Serendipitously, the dye is not only in the right place to promote LPO by means of light activation, but also benefits from the LD microenvironment itself. This provides a sort of *spatiofunctional* control to the PS, which adds to the *spatiotemporal* control inherent to light-activated processes.

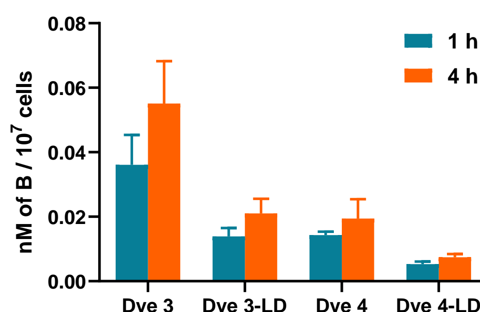

Figure 4. Cellular and LD uptake of **3** and **4** in U87 cells determined by ICP-MS.

Considering these results, we addressed if the photosensitizing action of **3** and **4** could trigger ferroptotic cell death through localized LPO in LDs. To elucidate this mechanism, we performed PDT assays using the well-known LPO inhibitor DL-α-tocopherol[29] and the ferroptosis inhibitor Ferrostatin-1 (Fer-1)[30] in combination with dye **3** and **4** at isotoxic concentrations (i.e., 10 and 300 nM, respectively). As shown in Figure 5, both DL-α-tocopherol and Fer-1 increased the cell

https://doi.org/10.26434/chemrxiv-2023-03s0m ORCID: https://orcid.org/0000-0002-7698-630X Content not peer-reviewed by ChemRxiv. License: CC BY-NC-ND 4.0

viability, suggesting that ferroptosis contributes significantly to the cell death induced by the PS activity of **3** and **4**. Additionally, we evaluated whether LDs could be involved in this process. The cytosolic phospholipase A2 alpha (cPLA2α) is a key enzyme in the process of lipid droplet formation.[31,32] We used pyrrolidine-2, a known inhibitor of this enzyme,[33,34] to further examine whether reducing the formation of lipid droplets could have an impact on the phototoxicity of **3** and **4** (Figure 5). The treatment with pyrrolidine-2 resulted in a significant increase in cell viability, which is consistent with our initial assumption that the accumulation of these dyes in LDs could enhance LPO and ferroptosis upon photosensitization.

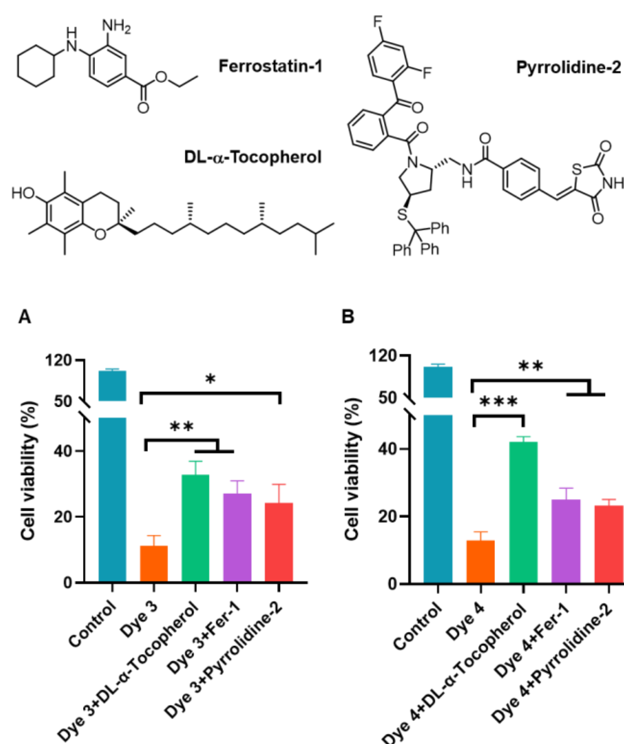

Figure 5. Cell viability of U87 cells determined upon co-incubation with (a) **3** (10 nM) or (b) **4** (300 nM) and different inhibitors. The ferroptosis inhibitor Fer-1, the lipid peroxidation inhibitor DL-α-Tocopherol, and the LD formation inhibitor pyrrolidine-2 were added at a final concentration of 50 μM, 100 μM, and 3 μM, respectively. Fer-1 and DL-α-Tocopherol were administered 1 h before co-incubation with the PSs, while pyrrolidine-2 was co-incubated with the PSs. Data are presented as mean ± SD (n = 3). (*P < 0.05, **P < 0.01, and ***P < 0.001, t-test).

Motivated by the observed potency and high phototoxicity indexes in cellular PDT experiments using the dyes **3** and **4**, we assessed the safety of these compounds *in vivo* using zebrafish embryos (*Danio rerio*). Zebrafish embryos are widely employed as a phenotype-based toxicity model in preclinical studies.[35–39] The lethality, hatching rates, and gross morphology were observed every 24 h for 4 days post-fertilization (dpf) following treatment with the compound in the dark. The compounds were administered into the fish water at 4 h post-fertilization and renewed after 48 h. At 4 dpf, dyes **3** and **4** were primarily localized in the yolk. They do not display apparent toxicity at concentrations up to 10 μM (Figure 6 A). Notably, the hatching rates of embryos exposed to these compounds remained unaltered, in contrast to cisplatin at comparable or even lower concentrations, as previously reported by our research groups.[40,41] The absence of dark toxicity at 10 μM provided significant encouragement for further *in vivo* investigations.

To explore the full potential of our compounds, we decided to increase the dye concentration administered to the zebrafish to 20 μM. At this significantly higher concentration, we observed some dark toxicity for **3**. However, it is plausible that this toxicity resulted from the exposure to microscope light every 24 h. In contrast, no dark toxicity was observed for **4**, potentially due to its observed less efficient cellular uptake (see above). Subsequently, the dyes **3** and **4** were subjected to an *in vivo* PDT assay, in which the zebrafish embryos were irradiated (488 nm) at 4 dpf for 10 or 20 min. The phenotypic consequences of this irradiation were then assessed at 7 dpf. Both compounds did not induce morphological changes at 10 μM. However, at 20 μM significant deformities/abnormalities in the phenotype (such as heart oedema) were observed for both compounds (see Figure 6 B and C with representative data for the example of dye **4**).

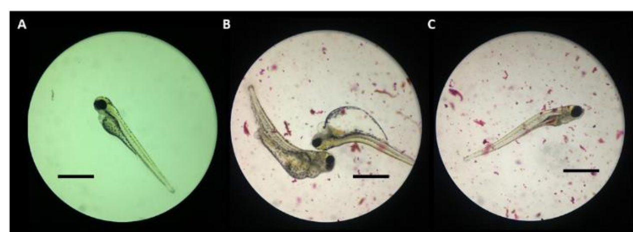

Figure 6. A – Normal phenotype at 3 dpf with incubation of dye **4** (1 μM). B and C – Typical abnormalities observed at 7 dpf with incubation of dye **4** (20 μM) and irradiation for 10 min at 488 nm at 4 dpf. Scale bars are 0.01 mm.

Conclusion

In conclusion, we investigated the potential of BASHY dyes as photosensitizers to promote PDT-induced ferroptosis in cancer cells. As we have shown, the excited triplet state population and singlet oxygen generation of the BASHY dyes is controlled by the delicate balance of CT and cyanine-like character. Using confocal microscopy, we confirmed their efficient accumulation in LDs and this feature, in combination with their efficient singlet oxygen generation, makes BASHY dyes ideally suited to promote LPO and ferroptosis. Of the four evaluated dyes, BASHY **3** was the most promising, displaying pronounced phototoxicity in the nanomolar range against the human glioblastoma multiform U87 cancer cell line, while showing virtually no dark toxicity. The resulting phototoxicity index, for which we can state a lower limit of 22700, is among the highest reported values and promotes this dye to gold-standard level. Gratifyingly, the accumulation of dye **3** in LDs was correlated with enhanced cell death, suggesting the involvement of localized LPO and ferroptotic pathways. These were indeed corroborated by a series of control experiments, using inhibitors of LPO and ferroptosis. In contrast, a derivative dye (dye **4**) with

https://doi.org/10.26434/chemrxiv-2023-03s0m **ORCID:** https://orcid.org/0000-0002-7698-630X Content not peer-reviewed by ChemRxiv. **License:** CC BY-NC-ND 4.0

limited LDs accumulation showed decreased PDT potency. The herein presented BASHY dye platform opens new avenues for the development of innovative therapeutic approaches in cancer treatment. The structural and electronic modularity of this exciting platform favors the functional extension of these tailored PS with view on introducing director groups for certain cancer cell lines or specific cell compartments.

Supporting Information

The authors have cited additional references within the Supporting Information.[42–53]

Acknowledgements

The authors acknowledge the financial support from Fundação para a Ciência e a Tecnologia, Ministério da Ciência e da Tecnologia, Portugal (SFRH/BD/132710/2017 to M.J.S.A.S., 2021.04125.CEECIND to F.M.F.S., 2022.06817.CEECIND to J.P.M.A.). The Research Institute for Medicines (iMed.ULisboa) acknowledges the financial support of Fundação para a Ciência e Tecnologia (projects PTDC/QUI-OUT/3989/2021; UIDB/04138/2020 and UIDP/04138/2020). The NMR spectrometers are part of the National NMR Network (PTNMR) and are partially supported by Infrastructure Project Nº 022161 (co-financed by FEDER through COMPETE 2020, POCI and PORL and FCT through PIDDAC). We thank the Spanish Ministry of Science and Innovation (PID2020-119992GB-I00 for U.P.; PID2019-104293GB-I00 for F.N.; PID2019-110441RB-C33 for F.B.), the Valencian Agency for Innovation (INNEST/2021/75 for F.B.), and the University of Huelva/Junta de Andalucía (UHU202070 for U.P.) for support. Further, we are indebted to the Supercomputing and Bioinformatics Centre (SCBI) of the University of Malaga for providing the computer resources used for the theoretical calculations. Y. Z. thanks the China Scholarship Council for funding. This work was also financially supported by an ERC Consolidator Grant PhotoMedMet to G.G. (GA 681679), by Qlife prématuration funding (G.G. and R.V.) and has received support under the program “Investissements d’Avenir” launched by the French Government and implemented by the ANR with the reference ANR-10-IDEX-0001-02 PSL (G.G.). L.G.G. thanks the ENS-PSL for her PhD fellowship. We thank Francisco Germán Blandón (Univ. Huelva) for technical support. LG thanks the École Normale Supérieure – PSL for her PhD fellowship. This study was supported by the Fond de Recherche du Québec - Nature et Technologies (FRQNT - Samuel-de-Champlain; LG, KC, AC, GG & SP), the Canada Foundation for Innovation (CFI; SP & AC) and the Natural Sciences and Engineering Research Council of Canada (NSERC; SP & AC). SP holds a Fond de Recherche du Québec - Santé (FRQS) Junior 2 research scholar award and the Anna Sforza Djoukhadjian Research Chair

Keywords: BASHY dyes; photodynamic therapy; cancer; lipid droplets; ferroptosis

References

[1] J. Li, F. Cao, H. Yin, Z. Huang, Z. Lin, N. Mao, B. Sun, G. Wang, *Cell Death Dis.* **2020**, *11*, 88.

[2] W. S. Yang, B. R. Stockwell, *Trends Cell Biol.* **2016**, *26*, 165–176.

[3] S. J. Dixon, B. R. Stockwell, *Nat. Chem. Biol.* **2014**, *10*, 9–17.

[4] F. Ursini, M. Maiorino, *Free Radic. Biol. Med.* **2020**, *152*, 175–185.

[5] A. N. von Krusenstiern, R. N. Robson, N. Qian, B. Qiu, F. Hu, E. Reznik, N. Smith, F. Zandkarimi, V. M. Estes, M. Dupont, T. Hirschhorn, M. S. Shchepinov, W. Min, K. A. Woerpel, B. R. Stockwell, *Nat. Chem. Biol.* **2023**, *19*, 719–730.

[6] H. Nakamura, K. Takada, *Cancer Sci.* **2021**, *112*, 3945–3952.

[7] T. Mishchenko, I. Balalaeva, A. Gorokhova, M. Vedunova, D. V. Krysko, *Cell Death Dis.* **2022**, *13*, 455.

[8] T. A. Mishchenko, I. V. Balalaeva, M. V. Vedunova, D. V. Krysko, *Trends Cancer* **2021**, *7*, 484–487.

[9] S. Shui, Z. Zhao, H. Wang, M. Conrad, G. Liu, *Redox Biol.* **2021**, *45*, 102056.

[10] H. Yuan, Z. Han, Y. Chen, F. Qi, H. Fang, Z. Guo, S. Zhang, W. He, *Angew. Chem. Int. Ed.* **2021**, *60*, 8174–8181.

[11] J. Zhang, L. Liu, X. Li, X. Shen, G. Yang, Y. Deng, Z. Hu, J. Zhang, Y. Lu, *Photodiagnosis Photodyn. Ther.* **2023**, *42*, 103612.

[12] S. Shui, Z. Zhao, H. Wang, M. Conrad, G. Liu, *Redox Biol.* **2021**, *45*, 102056.

[13] V. G. Jiménez, F. M. F. Santos, S. Castro-Fernández, J. M. Cuerva, P. M. P. Gois, U. Pischel, A. G. Campaña, *J. Org. Chem* .**2018**, *83*, 14057–14062.

[14] F. M. F. Santos, Z. Domínguez, M. M. Alcaide, A. I. Matos, H. F. Florindo, N. R. Candeias, P. M. P. Gois, U. Pischel, *ChemPhotoChem* **2018**, *2*, 1038–1045.

[15] M. M. Alcaide, F. M. F. Santos, V. F. Pais, J. I. Carvalho, D. Collado, E. Pérez-Inestrosa, J. F. Arteaga, F. Boscá, P. M. P. Gois, U. Pischel, *J. Org. Chem.* **2017**, *82*, 7151–7158.

[16] F. M. F. Santos, Z. Domínguez, J. P. L. Fernandes, C. Parente Carvalho, D. Collado, E. Pérez-Inestrosa, M. V. Pinto, A. Fernandes, J. F. Arteaga, U. Pischel, P. M. P. Gois, *Chem. Eur. J.* **2020**, *26*, 14064–14069.

[17] J. Felicidade, F. M. F. Santos, J. F. Arteaga, P. Remón, R. Campos-González, H. Nguyen, F. Nájera, F. Boscá, D. Y. W. Ng, P. M. P. Gois, U. Pischel, *Chem. Eur. J.* **2023**, *29*, e202300579.

[18] F. M. F. Santos, J. N. Rosa, N. R. Candeias, C. P. Carvalho, A. I. Matos, A. E. Ventura, H. F. Florindo, L. C. Silva, U. Pischel, P. M. P. Gois, *Chem. Eur. J.* **2016**, *22*, 1631–1637.

[19] J. A. Olzmann, P. Carvalho, *Nat. Rev. Mol. Cell. Biol.* **2019**, *20*, 137–155.

[20] A. D. Laurent, B. Le Guennic, D. Jacquemin, *Theor. Chem. Acc.* **2016**, *135*, 173.

[21] M. A. Filatov, *Org. Biomol. Chem.* **2020**, *18*, 10–27.

[22] M. S. Baptista, J. Cadet, P. Di Mascio, A. A. Ghogare, A. Greer, M. R. Hamblin, C. Lorente, S. C. Nunez, M. S. Ribeiro, A. H. Thomas, M. Vignoni, T. M. Yoshimura, *Photochem. Photobiol.* **2017**, *93*, 912–919.

[23] V.-N. Nguyen, Y. Yan, J. Zhao, J. Yoon, *Acc. Chem. Res.* **2021**, *54*, 207–220.

[24] R. R. Nani, J. A. Kelley, J. Ivanic, M. J. Schnermann, *Chem. Sci.* **2015**, *6*, 6556–6563.

https://doi.org/10.26434/chemrxiv-2023-03s0m **ORCID:** https://orcid.org/0000-0002-7698-630X Content not peer-reviewed by ChemRxiv. **License:** CC BY-NC-ND 4.0

[25] L. Schneider, M. Kalt, S. Koch, S. Sithamparanathan, V. Villiger, J. Mattiat, F. Kradolfer, E. Slyshkina, S. Luber, M. Bonmarin, C. Maake, B. Spingler, *J. Am. Chem. Soc.* **2023**, *145*, 4534–4544.

[26] J. A. Roque, P. C. Barrett, H. D. Cole, L. M. Lifshits, G. Shi, S. Monro, D. von Dohlen, S. Kim, N. Russo, G. Deep, C. G. Cameron, M. E. Alberto, S. A. McFarland, *Chem. Sci.* **2020**, *11*, 9784–9806.

[27] B. G. Tenchov, R. C. MacDonald, D. P. Siegel, *Biophys. J.* **2006**, *91*, 2508–2516.

[28] S. Patel, N. Ashwanikumar, E. Robinson, Y. Xia, C. Mihai, J. P. Griffith, S. Hou, A. A. Esposito, T. Ketova, K. Welsher, J. L. Joyal, Ö. Almarsson, G. Sahay, *Nat. Commun.* **2020**, *11*, 983.

[29] N. Barouh, C. Bourlieu-Lacanal, M. C. Figueroa-Espinoza, E. Durand, P. Villeneuve, *Compr. Rev. Food Sci. Food Saf.* **2022**, *21*, 642–688.

[30] G. Miotto, M. Rossetto, M. L. Di Paolo, L. Orian, R. Venerando, A. Roveri, A.-M. Vučković, V. Bosello Travain, M. Zaccarin, L. Zennaro, M. Maiorino, S. Toppo, F. Ursini, G. Cozza, *Redox Biol.* **2020**, *28*, 101328.

[31] L.-L. Lin, M. Wartmann, A. Y. Lin, J. L. Knopf, A. Seth, R. J. Davis, *Cell* **1993**, *72*, 269–278.

[32] A. Zadoorian, X. Du, H. Yang, *Nat. Rev. Endocrinol.* **2023**, *19*, 443–459.

[33] I. Zhang, Y. Cui, A. Amiri, Y. Ding, R. E. Campbell, D. Maysinger, *Eur. J. Pharm. Biopharm.* **2016**, *100*, 66–76.

[34] A. M. Astudillo, J. P. Rodríguez, C. Guijas, J. M. Rubio, M. A. Balboa, J. Balsinde, *Cells* **2021**, *10*, 447.

[35] J. M. Spitsbergen, M. L. Kent, *Toxicol. Pathol.* **2003**, *31*, 62–87.

[36] A. L. Rubinstein, *Expert Opin. Drug Metab. Toxicol.* **2006**, *2*, 231–240.

[37] F. M. Richards, W. K. Alderton, G. M. Kimber, Z. Liu, I. Strang, W. S. Redfern, J.-P. Valentin, M. J. Winter, T. H. Hutchinson, *J. Pharmacol. Toxicol. Methods* **2008**, *58*, 50–58.

[38] N. Mandrekar, N. L. Thakur, *Biotechnol. Lett.* **2009**, *31*, 171–179.

[39] C. A. MacRae, R. T. Peterson, *Nat. Rev. Drug. Discov.* **2015**, *14*, 721–731.

[40] M. Haghdoost, G. Golbaghi, M. Létourneau, S. A. Patten, A. Castonguay, *Eur. J. Med. Chem.* **2017**, *132*, 282–293.

[41] G. Golbaghi, M. M. Haghdoost, D. Yancu, Y. López de los Santos, N. Doucet, S. A. Patten, J. T. Sanderson, A. Castonguay, *Organometallics* **2019**, *38*, 702–711.

[42] A. D. Becke, *J. Chem. Phys.* **1993**, *98*, 5648–5652.

[43] T. Yanai, D. P. Tew, N. C. Handy, *Chem. Phys. Lett.* **2004**, *393*, 51–57.

[44] C. Adamo, V. Barone, *J. Chem. Phys.* **1999**, *110*, 6158–6170.

[45] J. Tomasi, B. Mennucci, R. Cammi, *Chem. Rev.* **2005**, *105*, 2999–3094.

[46] Z. Liu, T. Lu, Q. Chen, *Carbon* **2020**, *165*, 461–467.

[47] Y. Zhao, D. G. Truhlar, *Theor. Chem. Acc.* **2008**, *120*, 215–241.

[48] T. Lu, F. Chen, *J. Comput. Chem.* **2012**, *33*, 580–592.

[49] S. Acheampong, M. Savva, *J. Biophys. Chem.* **2011**, *02*, 53–62.

[50] I. Carmichael, G. L. Hug, *J. Phys. Chem. Ref. Data* **1986**, *15*, 1–250.

[51] R. V. Bensasson, J.-C. Gramain, *J. Chem. Soc., Faraday Trans. 1* **1980**, *76*, 1801.

[52] C. Grewer, H. D. Brauer, *J. Phys. Chem.* **1993**, *97*, 5001–5006.

[53] Gaussian 16, Revision C.01, M. J. Frisch, G. W. Trucks, H. B. Schlegel, G. E. Scuseria, M. A. Robb, J. R. Cheeseman, G. Scalmani, V. Barone, G. A. Petersson, H. Nakatsuji, X. Li, M. Caricato, A. V. Marenich, J. Bloino, B. G. Janesko, R. Gomperts, B. Mennucci, H. P. Hratchian, J. V. Ortiz, A. F. Izmaylov, J. L. Sonnenberg, D. Williams-Young, F. Ding, F. Lipparini, F. Egidi, J. Goings, B. Peng, A. Petrone, T. Henderson, D. Ranasinghe, V. G. Zakrzewski, J. Gao, N. Rega, G. Zheng, W. Liang, M. Hada, M. Ehara, K. Toyota, R. Fukuda, J. Hasegawa, M. Ishida, T. Nakajima, Y. Honda, O. Kitao, H. Nakai, T. Vreven, K. Throssell, J. A. Montgomery, Jr., J. E. Peralta, F. Ogliaro, M. J. Bearpark, J. J. Heyd, E. N. Brothers, K. N. Kudin, V. N. Staroverov, T. A. Keith, R. Kobayashi, J. Normand, K. Raghavachari, A. P. Rendell, J. C. Burant, S. S. Iyengar, J. Tomasi, M. Cossi, J. M. Millam, M. Klene, C. Adamo, R. Cammi, J. W. Ochterski, R. L. Martin, K. Morokuma, O. Farkas, J. B. Foresman, and D. J. Fox, Gaussian, Inc., Wallingford CT, 2016.

https://doi.org/10.26434/chemrxiv-2023-03s0m **ORCID:** https://orcid.org/0000-0002-7698-630X Content not peer-reviewed by ChemRxiv. **License:** CC BY-NC-ND 4.0

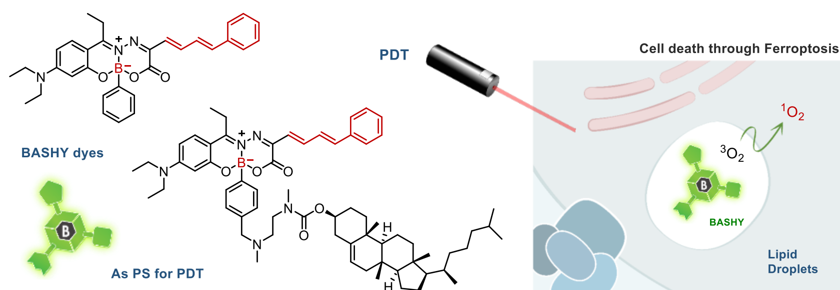

Boronic acid derived salicylidenehydrazone (BASHY) dyes are highly efficient singlet-oxygen photosensitizers (PSs; Φ_Δ up to 0.8) that induce ferroptosis in cancer cells triggered by photodynamic therapy.

Institute and/or researcher Twitter usernames: @GoisLab; @GasserGroup; @LabPischel

https://doi.org/10.26434/chemrxiv-2023-03s0m ORCID: https://orcid.org/0000-0002-7698-630X Content not peer-reviewed by ChemRxiv. License: CC BY-NC-ND 4.0